

A Century of Solar Ca II Measurements and Their Implication for Solar UV Driving of Climate

**Peter Foukal · Luca Bertello · William C. Livingston ·
Alexei A. Pevtsov · Jagdev Singh · Andrey G. Tlatov ·
Roger K. Ulrich**

Received: 16 November 2008 / Accepted: 5 February 2009 / Published online: 5 March 2009
© The Author(s) 2009. This article is published with open access at Springerlink.com

Abstract Spectroheliograms and disk-integrated flux monitoring in the strong resonance line of Ca II (K line) provide the longest record of chromospheric magnetic plages. We compare recent reductions of the Ca II K spectroheliograms obtained since 1907 at the Kodaikanal, Mt. Wilson, and US National Solar Observatories. Certain differences between the individual plage indices appear to be caused mainly by differences in the spectral passbands used. Our main finding is that the indices show remarkably consistent behavior on the multidecadal time scales of greatest interest to global warming studies. The reconstruction of

P. Foukal (✉)
Heliophysics, Inc., 192 Willow Road, Nahant, MA 01908, USA
e-mail: pvfoukal@comcast.net

L. Bertello · R.K. Ulrich
Department of Physics and Astronomy, University of California at Los Angeles, Los Angeles,
CA 90095-1547, USA

L. Bertello
e-mail: bertello@astro.ucla.edu

R.K. Ulrich
e-mail: ulrich@astro.ucla.edu

W.C. Livingston
National Solar Observatory, Tucson, AZ 85726, USA
e-mail: wcl@noao.edu

A.A. Pevtsov
National Solar Observatory, Sunspot, NM 88349, USA
e-mail: apevtsov@nso.edu

J. Singh
Indian Institute of Astrophysics, Koramangala, Bangalore, India
e-mail: jsingh@iiap.res.in

A.G. Tlatov
Kislovodsk Solar Station of Pulkovo Observatory, Kislovodsk, Russia
e-mail: tlatov@mail.ru

solar ultraviolet flux variation from these indices differs significantly from the 20th-century global temperature record. This difference is consistent with other findings that, although solar UV irradiance variation may affect climate through influence on precipitation and storm tracks, its significance in global temperature remains elusive.

Keywords Solar activity · Magnetic plages · Solar ultraviolet irradiance · Sun – climate effects

1. Introduction

Solar magnetic plages and network are most easily observed in the strong chromospheric absorption lines, such as the resonance line of Ca II (called Ca II K) in the violet at 393.37 nm, which is the strongest solar spectral line observable from the ground. Consequently, photographic imaging in this K line has provided an important measure of solar magnetic activity since the earliest spectroheliograms were obtained by H. Deslandres in France and by G.E. Hale in the USA in the early 1890s.

Archives of daily spectroheliograms maintained at Kodaikanal Observatory, India, since 1907 and at Mt. Wilson Observatory, USA, since 1915 provide the longest available record of the daily changing structure of magnetic plages and active network. Spectroheliograms compiled since 1965 and disk-integrated K-line fluxes measured since 1974 at the National Solar Observatory provide both supplementary and complementary information. Other shorter spectroheliogram time series (*e.g.*, Arcetri, Italy; Meudon, France; and Kislovodsk, Russia) also enhance the record.

These archives are of great importance because the plages account for roughly one-half of the Sun's total magnetic flux (*e.g.*, Schrijver and Harvey, 1989) and for most of the Sun's variability in ultraviolet flux (*e.g.*, Lean, 1987; Solanki and Unruh, 1998) and in 1-year variation of total irradiance (*e.g.*, Foukal and Lean, 1988). K-line observations between 1947 and 1984 at McMath Hulbert Observatory, for instance, used to measure daily plage areas and intensities (Swartz and Overbeck, 1971), served to estimate the Sun's ultraviolet (UV) and extreme ultraviolet (EUV) flux variation and its effects on the Earth's upper atmosphere. More recently, the 20th-century plage record has been used to test the effectiveness of solar UV driving of climate (Foukal, 2002; Foukal, Chulsky, and Weisenstein, 2008).

We provide here a brief description of these Ca II K databases and their reduction, compare the results, and describe an immediate application to Sun – climate studies. A companion paper (Tlatov, Pevtsov, and Singh, 2009; referred to henceforth as Paper 2) focuses on the reduction procedures used by these authors in their analysis of the Kodaikanal, Mt. Wilson, and Sacramento Peak spectroheliograms, the results of which are included in this present paper.

2. Data

2.1. Mt. Wilson Data

The daily Mt. Wilson Observatory (MWO) Ca II K images analyzed here were obtained between 1915 and 1985 at the 60-foot tower and spectroheliograph. Calibration wedges were not imprinted until after 1961. The nominal spectral passband was approximately 0.02 nm. The images were first digitized by Cambridge Research and Instrumentation, Inc. (CRI), using a 512-pixel format, 8-bit camera (Foukal, 1996) and are available from the National Geophysical Data Center (NGDC).

During the CRI reduction it was soon recognized that calibrations with the imprinted wedges were of limited use, even when these were available. For instance, their density range often did not extend over the full range of plage intensity. Attempts to use the known solar limb darkening in the K line as a density calibration for the plates taken prior to 1961 were also unsuccessful.

Correlations of plage areas with other solar activity indices such as sunspot number and the 10.7-cm microwave flux, F10.7, showed that weighting of the areas by plage intensity increased the scatter in the regression curves, rather than improving the correlation. Since the F10.7 index varies as the product of plage area times brightness, the correlation should improve if the K-line plage brightness is also taken into account. The finding that it does not indicated that real variations in plage brightness were masked by brightness measurement errors caused mainly by the calibration uncertainty. Therefore, subsequent reduction focused on *relative changes in plage area*, rather than on their brightness. This emphasis on area variation is supported by other analyses (*e.g.*, Worden, White, and Woods, 1998) in which no trends in plage brightness that might affect the plage contribution to irradiance variation over the 11-year cycle were found.

Initial inspection of the plates showed that scratches and development inhomogeneities, variable vignetting, and noncircular images would introduce difficulties into the reduction. This suggested that an interactive approach might be more successful than using fully automated software, even if it introduced some operator judgment. Therefore, interactive software was developed at CRI to remove limb darkening, establish quiet-Sun thresholds, and measure the areas of active region plages corrected for foreshortening. This first reduction produced a time series of active region plage areas for the period 1915–1984 (Foukal, 1996).

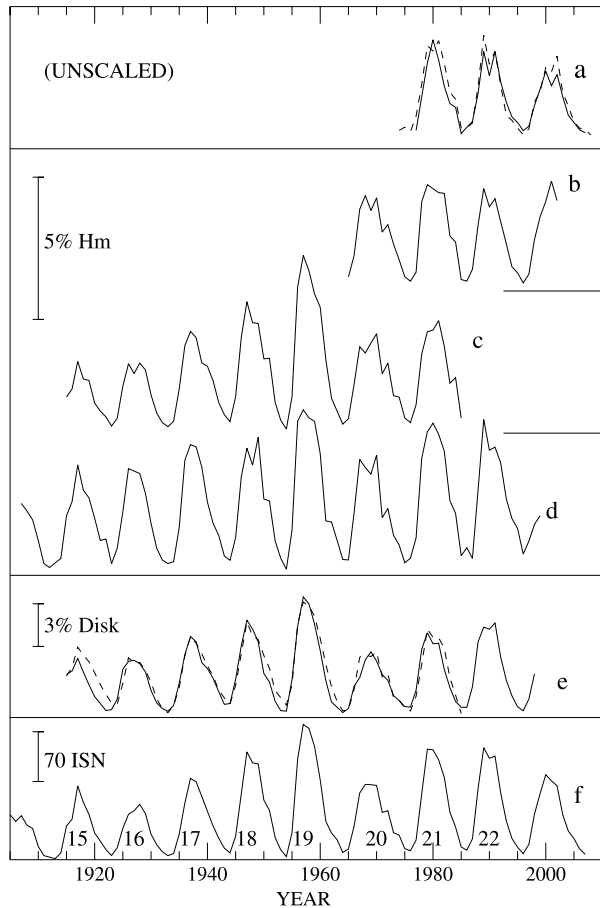
However, modeling of solar irradiance variation requires the contribution not only of active region plages but also of the enhanced network. To provide this, the data were reduced a second time at CRI to include the enhanced network areas. The reduction was also extended from 1985 to 1999 by digitizing four evenly spaced plates per month from the National Solar Observatory/Sacramento Peak Observatory (NSO/SPO) spectroheliogram archive. This time series, called Apn (Foukal, 1998), is reproduced here in Figure 1(e), as annual averages of the foreshortened (as required in irradiance analyses) plage and active network areas in percent of the solar disk.

The same data were redigitized a few years later at the University of California, Los Angeles (UCLA), by using a higher resolution (3000×3000), 12-bit digitizer (Lefebvre *et al.*, 2005). An important objective was to reproduce the Mt. Wilson images and log books archivally at their full resolution. The data have also been used to study the solar rotation profile and magnetic field strength variation.

In this UCLA reduction, vignetting and limb darkening were removed in two ways. In one approach, applied to all data between 1915 and 1985, median filtering was used to produce a low-pass image. In the second approach, used on data after 1961 (for which calibration wedges were available) the data were fitted to both a vignetting function and a limb-darkening function. However, the calibration uncertainties encountered in the earlier CRI reduction were found to also limit the accuracy of area and brightness measurements of the K-line structures in the UCLA analysis.

The UCLA K-line index was determined by using a multistep procedure. First, the original image was divided by its corresponding low-pass-filtered version to produce an intensity ratio image in which the background has a typical value of unity. Second, a histogram was calculated using pixels located within 0.97 solar radii from the center of the image. The width and the center of this distribution were determined from a Gaussian fit to the histogram by using an equal number of bins around the maximum of the distribution. This choice of

Figure 1 Time series of annual mean plage indices from (a) Sun as a star (SPO, solid line; KPO, dashed line) and spectroheliogram-based indices from (b) SPO (Paper 2), (c) MWO (Paper 2), (d) Kodaikanal (Paper 2), and (e) Apn (solid line) and UCLA (dashed line). (f) Annual mean international sunspot number (ISN). Scales indicated by bars show percent of the hemisphere area for panels (b), (c), and (d) and percent of disk area for panel (e).



parameters limited the analysis to the central part of the histogram, which is well described by a Gaussian function. Finally, the calculated width was used to define the boundaries of a new histogram calculated from the distribution of values in the intensity ratio image, using only pixel values in the range. A four-parameter Gaussian function was used to model this distribution and the value of the constant baseline was defined to be the index of K-line plages and active network.

Indices calculated from individual spectroheliograms have been averaged together to produce a time series of annual means for this UCLA plage index, which is also plotted (dashed line) in Figure 1(e). The number of images used to calculate these mean values varies significantly from year to year, from as low as 140 in 1915 to about 1100 in 1946. The calculated rms of the mean values, however, is consistent over time and is typically below 1%.

The MWO/UCLA digital data were also reduced independently by Tlatov and Pevtsov, as described in the accompanying Paper 2. This plage index, plotted in Figure 1(c), again measures plage area in active regions and enhanced network.

2.2. Kodaikanal Data

Daily K-line spectroheliograms were obtained at Kodaikanal Observatory, India, between 1907 and 1999. The 0.05-nm spectral passband is significantly wider than that used

for the Mt. Wilson observations, so the structures measured are noticeably different. For instance, sunspots are much more visible, and plages are imaged lower in the atmosphere, so their area is smaller. Dark disk filaments, visible in the MWO images, are not seen.

The 26 640 images in this archive provide the longest and probably most homogeneous Ca II K database (Ermolli *et al.*, 2007). The images have been digitized with 8-bit density resolution and approximately 1400-pixel resolution by Tlatov, Pevtsov, and Singh (Paper 2). Their reduction followed a similar approach to that which they used for the Mt. Wilson data. The results are shown in Figure 1(d). A new digitizer using a 4000×4000 pixel format CCD camera and 16-bit density resolution has more recently become available at Kodaikanal Observatory for future re-digitization of this plate archive.

2.3. NSO/SPO Spectroheliogram Data

Daily K-line spectroheliograms were also obtained at Sacramento Peak Observatory, USA, between 1965 and 2002, with a nominally 0.05-nm spectral passband. Initially, four images per month (spaced as evenly as the data enabled) in the period 1985–1999 were digitized at 512-pixel, 8-bit resolution (Foukal, 1998). These are included in the Apn time series plotted in Figure 1. A complete digitization of the entire collection of 6033 plates was carried out later with 1500-pixel, 16-bit resolution (Paper 2). These data were reduced, as described in that accompanying paper, for the Mt. Wilson images. They are plotted in Figure 1(b).

2.4. NSO Sun-as-a-Star Data

In addition to these spectroheliograms, the Sun's emission in a 0.1-nm K-line passband has also been monitored in disk-integrated light. These observations were made on an approximately daily basis from SPO between 1977 and 2007 and (using a different instrumental arrangement) from Kitt Peak Observatory (KPO) on a 2–3 image month⁻¹ basis since 1974 (Livingston *et al.*, 2007). Comparison of results obtained using all days of observation versus only those days when both SP and KPO data are available shows that the sparseness and irregularity of these Sun-as-a-star data can affect their annual means. These data are now being obtained daily using the new NSO SOLIS instrument since 2007. This record is plotted in Figure 1(a).

3. Results and Errors

Figure 1 shows the six time series of annual mean plage index. Also shown are the corresponding annual mean sunspot numbers, in Figure 1(f). Although the plage indices plotted in the five imaging records are defined somewhat differently, they measure essentially the same quantity – the area of plages including the “enhanced” (or “active”) network. The Sun-as-a-star index differs in recording brightness, as well as area changes. Scatter plots comparing the five spectroheliogram-based records exhibit correlation coefficients exceeding 0.95, which is not surprising since they are all quasi-sinusoids matched in both period and phase.

It can be seen from Figure 1 that, although differences exist between the detailed shapes of the 11-year cycles, their ordering by amplitude (*i.e.*, rank ordering) in the three separate

reductions of the MWO data (Figures 1(c) and (e)) agrees well. However, there are significant differences between these results from the MWO data compared to the Kodaikanal data. For example, whereas cycle 19 is the strongest in all the time series, its relative amplitude is significantly lower in the Kodaikanal data (Figure 1(d)) than in the MWO data. Cycle 18 is also weaker. Cycle 21, in contrast, is stronger than in the MWO results.

Comparison of the SPO index (Figure 1(b)) over its shorter overlap with Apn and Kodaikanal shows similar differences. That is, there is rough agreement in relative amplitudes of cycles 20, 21, and 22 with the Kodaikanal index, but there is disagreement over these cycles with Apn. When it is compared with the Sun-as-a-star index (Figure 1(a)), the amplitudes match for cycles 21 and 22 but its amplitude for cycle 23 is much higher.

It is useful to compare the behavior of these Ca II K time series with the sunspot number, since this index has been most widely used in the past as a proxy of plage area in studies of solar activity, of UV solar irradiance extending earlier than the beginning of the 10.7-cm microwave flux in 1947 (*e.g.*, Lean, Beer, and Bradley, 1995; Solanki and Fligge, 1998), and of total solar irradiance (TSI) earlier than the beginning of the Greenwich sunspot record in 1874 (Lean, Beer, and Bradley, 1995).

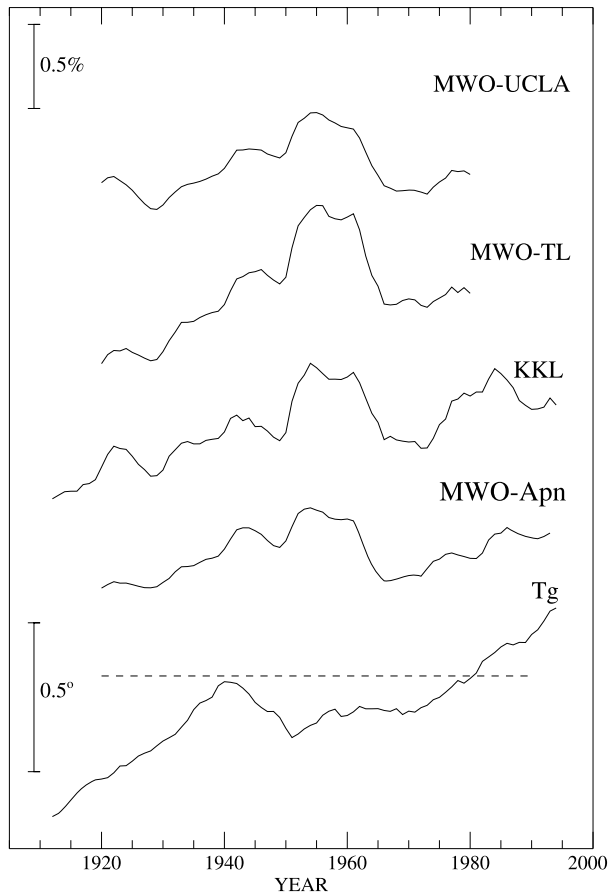
Correlations with the sunspot number plotted in Figure 1 exceed 0.95 for all the indices, and the rank ordering of the cycles in the three MWO-based indices agrees with their ordering in sunspot number. The ordering of the three cycles 21–23 measured in the Sun-as-a-star data also agrees with the ordering in spot number. For the two Kodaikanal- and SP-based indices the agreement with sunspot number is less satisfactory. Again, as before, cycles 18 and 19 are weaker, and cycle 21 is stronger, than in the sunspot number.

Some differences among the MWO, Kodaikanal, and SPO spectroheliograms help to explain this different rank ordering. As mentioned earlier (see also Ermolli *et al.*, 2007) the Kodaikanal and SPO observations were made in a wider spectral passband and so refer to a deeper level in the solar atmosphere where plage areas are smaller. The most likely explanation of the weaker cycles 18 and 19 is given in the accompanying Paper 2. They point out that spot areas are included in the narrower band MWO data, where they are difficult to identify and separate from plage (see also Foukal, 1993). Spots are much more easily identified in the wider band NSO and Kodaikanal data and are not included in those plage area time series.

Sampling differences could in principle also affect the comparison of the K-line data. However, they cannot be the main explanation of the weak cycles 18 and 19 seen in the Kodaikanal time series. The sampling in the spectroheliogram time series is much more frequent than in the Sun-as-a-star observations. During the cycle 18–19 time period, between approximately 1944 and 1964, the number of plates per year analyzed for the Mt. Wilson time series was at its highest, and never below 450 year^{-1} . The number of Kodaikanal plates year^{-1} analyzed was lower, but roughly constant and still approximately 250 year^{-1} . There is no evidence of extended sampling gaps in either of these spectroheliogram data sets that could explain why cycles 18 and 19 should disagree despite the good agreement during the rest of the period covered.

Figure 2 shows the four longest time series, based on observations from MWO and Kodaikanal, smoothed using an 11-year boxcar running mean. Both the MWO and Kodaikanal time series show the same broad maximum in plage index between the early 1950s and early 1960s. They also all show a general rise beginning around the mid 1920s toward a subsidiary maximum peaking around the early 1940s. Therefore, despite the differences in the annual average data just described, the four longest plage indices share certain robust features on a multidecadal time scale of greater interest in studies of possible variable solar influence on climate.

Figure 2 Time series of 11-year running means of plage indices from MWO (UCLA), MWO (Paper 2), Kodaikanal, and Apn. Also shown is the 11-year smoothed global temperature, T_g . The top scale refers to 0.5% variation in the four plage indices, and the bottom scale to 0.5°C in T_g .



4. Discussion and Conclusions

4.1. Behavior of Plage Indices

Comparison of the annual mean time series presented here shows good agreement between three independent reductions of the MWO archival K-line spectroheliograms for 1915–1984 by the CRI, UCLA, and Kislovodsk workers. This is noteworthy, given differences in definition of the three plage indices and in the thresholds used in their measurement. Significant differences do, however, exist in the rank ordering of activity cycle amplitudes when the same reduction technique is used on three different spectroheliogram sets from MWO, Kodaikanal, and NSO/SPO. The rank ordering in the NSO/SPO and Kodaikanal time series also differs from the ordering of cycles 21–23 observed in the Ca II K flux of the Sun considered as a star, as measured at NSO.

The rank ordering of the cycle amplitudes in the three reductions of the MWO-based plage indices is the same as in the time series of sunspot number. This holds also for the NSO Sun-as-a-star time series for the cycles 21–23 covered by those measurements. This agreement is consistent with the high correlation found (*e.g.*, Tapping, 1987) between sunspot number and the F10.7 microwave index, which measures plage and network area variation somewhat higher in the chromosphere and transition region than the K-line indices.

There is no *a priori* reason to assume that plage-related solar activity indices necessarily follow the sunspot number (if there were, measurement of plage data would have little value). For instance, the rank ordering of cycles measured in white-light faculae (which are the downward photospheric extension of the chromospheric plages studied here) is, surprisingly, the *inverse* of their ordering in sunspot number (Brown and Evans, 1980).

This surprising inverse ordering is a consequence of the increasing ratio of sunspot to facular area with increasing spot size in the Sun and in similar, but more active stars (Foukal, 1993). As explained there, this inverse ordering is seen in white-light faculae, which tend to be associated with the brightest, most recently emerged magnetic fields around the largest spots. It is masked in the time series of Ca II K plage areas, which are dominated by large, older plage remnants that are harder to detect in white light. Compared to the relatively modest faculae around the largest spots, these fainter plage areas are proportionately larger than the small spots with which they are associated. This is the main reason why the K line and F10.7-cm indices, which respond to the total plage area including the extended fainter plages, scale so linearly with sunspot number.

Therefore, it is significant that we are able to extend the period of agreement between directly measured plage indices and sunspot number back to 1915, thus by about 50% compared to the earlier period 1947–present offered by the F10.7 plage index. The agreement we see here between sunspot number and the MWO-based and Sun-as-a-star indices covering 1915–present increases confidence in use of the sunspot number to reconstruct the bright component of solar irradiance. The assumption that this proxy was valid underlies most reconstructions of the spot and facular contribution to variation in total solar irradiance (*e.g.*, Foukal and Lean, 1990; Lean, Beer, and Bradley, 1995; Solanki and Fligge, 1998) back to 1874 when spot area data become available, and in solar UV irradiance (*e.g.*, Lean, Beer, and Bradley, 1995) back to the beginning of sunspot number estimate availability after the early 17th century.

If one assumes that the interpretation of Paper 2 is correct, the weaker agreement with sunspot number found for the Kodaikanal and NSO/SPO time series carries interesting additional information. That is, the Kodaikanal and NSO time series should provide a better approximation to the *bright component* contribution to (a) UV variability at wavelengths that originate in the upper photosphere (including the important range between about 170 and 240 nm mainly responsible for ozone concentration) and to (b) the total solar irradiance. The MWO time series, however, would better represent the variability of shorter UV and EUV wavelengths that originate from the chromospheres and transition regions of both plages and spots, since spots become brighter than the photosphere in these radiations (Foukal *et al.*, 1974; Brueckner and Bartoe, 1974).

Our main finding is that, although differences exist between the annually averaged plage indices, they agree well on a multidecadal time scale of greatest interest to most Sun–climate studies. This is remarkable given the potential for calibration drifts from changes in dispersive element size and position, in spectral passband width, in exposure, in emulsion and development techniques, and also in vignetting and scattered light that have been described by Ermolli *et al.* (2007).

4.2. Application to Solar UV Forcing of Climate

To illustrate the usefulness of the K-line data for global warming studies, we compare in Figure 2 the 11-year smoothed plage indices with the similarly smoothed record of global temperature. The plage area variation drives the variation of UV flux in the spectral region shortward of approximately 240 nm. In this region the contrast of plages is sufficiently high

that their area variation determines the time behavior of the UV flux, with negligible contribution from sunspots (e.g., Lean, 1987; Solanki and Unruh, 1998). A study using a 2-D stratospheric chemistry model indicates that this wavelength range, rather than longer wavelengths (>240 nm, where spots *cannot* be neglected), is responsible for variation of ozone (Foukal, Chulsky, and Weisenstein, 2008). Therefore, the plage indices plotted here should provide a good estimate of 20th-century solar UV irradiance variation on the multidecadal time scale, in this ozone-effective spectral range.

We see that the smoothed plage indices and global temperature, T_g , differ significantly, particularly around the middle of the 20th century. Specifically, the major maximum in plage indices between the early 1950s and 1960s corresponds to the broad local *minimum* of T_g spanning roughly the early 1940s through 1970s. The ocean temperature record for the mid-20th century may be influenced by a recently identified change in measurement technique (Thompson *et al.*, 2008). This correction cannot, however, explain why the dominant peak seen in the plage indices is absent in T_g .

The correlation coefficients, r , between the 1-year smoothed plage time series and T_g lie between approximately $0.25 < r < 0.50$ over the overlap period 1915–1984 of the MWO and Kodaikanal plage indices. This period avoids the most recent two decades of steeply increasing global warming widely ascribed to anthropogenic influence. These relatively weak correlations suggest that no more than about 6%–25% of the naturally occurring 20th-century variance (r^2) in T_g is statistically ascribable to solar UV forcing.

The correlation of Apn and the Kodaikanal time series with T_g over their full extent to 1999 is greater ($r = 0.49$ and $r = 0.69$, respectively). However, this increased correlation (corresponding to fractions of the total variance between approximately 0.25 and 0.5) arises mainly from the slow upward trend in these two series seen in Figure 2. They share this slow upward rise with T_g when the anthropogenically affected recent decades are included.

The relatively low correlation between the dominant features seen in reconstructions of global temperature and UV irradiance seems to argue against strong solar UV driving of the global warming reported to have occurred since the 17th century. This finding appears to be consistent with recent modeling (Haigh, 1996; Haigh, Blackburn, and Day, 2005; Shindell *et al.*, 2001) that indicates that solar UV flux variation affects storm tracks and precipitation while having less effect on global temperature.

Acknowledgements PVF thanks Greg Chulsky for assistance in data analysis. He is also grateful to the Observatories of the Carnegie Institution of Washington for facilitating access to the MWO plate collection. Work on this research at Heliophysics, Inc., is supported by NSF Grant No. ATM 0718305. The National Solar Observatory is operated by the Association for Research in Astronomy (AURA, Inc.) under cooperative agreement with the National Science Foundation (NSF).

Open Access This article is distributed under the terms of the Creative Commons Attribution Noncommercial License which permits any noncommercial use, distribution, and reproduction in any medium, provided the original author(s) and source are credited.

References

- Brown, G.M., Evans, D.R.: 1980, *Solar Phys.* **66**, 233.
 Brueckner, G.E., Bartoe, J.-D.F.: 1974, *Solar Phys.* **38**, 133.
 Ermolli, I., Tlatov, A., Solanki, S.K., Krivova, N.A., Singh, J.: 2007, In: Heinzl, P., Dorotovic, I., Rutten, R. (eds.) *The Physics of Chromospheric Plasmas CS-368*, Astron. Soc. Pac., San Francisco, 533.
 Foukal, P.V., Huber, M.C.E., Noyes, R.W., Reeves, E.M., Schmahl, E.J., Timothy, J.G., Vernazza, J.E., Withbroe, G.L.: 1974, *Astrophys. J.* **193**, L143.
 Foukal, P.: 1993, *Solar Phys.* **148**, 219.

- Foukal, P.: 1996, *Geophys. Res. Lett.* **23**, 2169.
- Foukal, P.: 1998, *Geophys. Res. Lett.* **25**, 2909.
- Foukal, P.: 2002, *Geophys. Res. Lett.* **29**, 2089. doi:[10.1029/2002GL015474](https://doi.org/10.1029/2002GL015474).
- Foukal, P., Lean, J.: 1988, *Astrophys. J.* **328**, 347.
- Foukal, P., Lean, J.: 1990, *Science* **247**, 556.
- Foukal, P., Chulsky, G., Weissenstein, D.: 2008, AGU Spring Meeting Abstracts SP 53B-06.
- Haigh, J.D.: 1996, *Science* **272**, 981.
- Haigh, J.D., Blackburn, M., Day, R.: 2005, *J. Clim.* **18**, 3672.
- Lean, J.: 1987, *J. Geophys. Res.* **92**, 839.
- Lean, J., Beer, J., Bradley, R.: 1995, *Geophys. Res. Lett.* **22**, 3195.
- Lefebvre, S., Ulrich, R.K., Webster, L.S., Varadi, F., Javaraiah, L., Bertello, L., Werden, L., Boyden, J.E., Gilman, P.: 2005, *Mem. Soc. Astron. Ital.* **76**, 862.
- Livingston, W., Wallace, L., White, O.R., Giampapa, M.S.: 2007, *Astrophys. J.* **657**, 1137.
- Schrijver, C.J., Harvey, K.L.: 1989, *Astrophys. J.* **343**, 481.
- Shindell, D.T., Schmidt, G.A., Mann, M.E., Rind, D., Waple, A.: 2001, *Science* **294**, 2149.
- Solanki, S.K., Fligge, M.: 1998, *Geophys. Res. Lett.* **25**, 341.
- Solanki, S.K., Unruh, Y.C.: 1998, *Astron. Astrophys.* **329**, 747.
- Swartz, W., Overbeck, R.: 1971, Penn State Univ. Scientific Report 373.
- Tapping, K.F.: 1987, *J. Geophys. Res.* **92**, 829.
- Thompson, D.W.J., Kennedy, J.J., Wallace, J.M., Jones, P.D.: 2008, *Nature* **453**, 646.
- Tlatov, A.G., Pevtsov, A.A., Singh, J.: 2009, *Solar Phys.* doi:[10.1007/s11207-009-9326-9](https://doi.org/10.1007/s11207-009-9326-9).
- Worden, J.R., White, O.R., Woods, T.N.: 1998, *Astrophys. J.* **496**, 998.